ALS-Causing Protein TDP-43 Impairs SREBP2 Cholesterol Regulation

Naohiro Egawa
Kyoto University: Kyoto Daigaku
Yuishin Izumi
Tokushima University Hospital: Tokushima Daigaku Byoin
Itaru Tsuge
Kyoto University: Kyoto Daigaku
Koji Fujita
University of Tokushima - Shinkura Area: Tokushima Daigaku
Hitoshi Shimano
University of Tsukuba: Tsukuba Daigaku
Keiichi Izumikawa
Tokyo University of Agriculture Faculty of Applied Bioscience: Tokyo Nogyo Daigaku Oyo Seibutsu Kagakubu
Nobuhiro Takahashi
Tokyo University of Agriculture Faculty of Applied Bioscience: Tokyo Nogyo Daigaku Oyo Seibutsu Kagakubu
Kayoko Tsukita
Kyoto University: Kyoto Daigaku
Takako Enami
Kyoto University: Kyoto Daigaku
Masahiro Nakamura
Kyoto University: Kyoto Daigaku
Akira Watanabe
Kyoto University: Kyoto Daigaku
Motoko Naitoh
Kyoto University: Kyoto Daigaku
Shigehiko Suzuki
Kyoto University: Kyoto Daigaku
Tsuneyoshi Seki
Kobe University: Kobe Daigaku
Kazuhiro Kobayashi
Kobe University: Kobe Daigaku
Tatsushi Toda

The University of Tokyo: Tokyo Daigaku
Ryuji Kaji
University of Tokushima: Tokushima Daigaku
Ryosuke Takahashi
Kyoto University: Kyoto Daigaku
Haruhisa Inoue (haruhisa@cira.kyoto-u.ac.jp)
Kyoto University https://orcid.org/0000-0001-8270-4025

Research Article

Keywords: ALS, TDP-43, SREBP2, cholesterol, dyslipidemia, Reverse translational research

Posted Date: June 21st, 2021

DOI: https://doi.org/10.21203/rs.3.rs-608138/v1

Abstract

Dyslipidemia is correlated with the prognosis of amyotrophic lateral sclerosis (ALS), a fatal motor neuron disorder characterized pathologically by TAR DNA binding protein (TDP-43) inclusions. We investigated molecular mechanisms of lipid metabolism regulated by TDP-43 in ALS. Expression microarray and RNA deep sequencing (RNA-Seq) were performed using cell lines expressing doxycycline-inductive TDP-43. Gene expression and transcriptome profiling identified 434 significantly altered genes under high levels of TDP-43 (Tukey's test, $P < 0.05$) including sterol regulatory element-binding protein 2 (SREBP2), a master regulator of cholesterol homeostasis and its downstream genes. TDP-43 overexpression impaired SREBP2 transcriptional activity, leading to inhibition of cholesterol biosynthesis via the nutrient- and growth factor-responsive kinase mTOR Complex I (mTORC1). The amount of cholesterol was significantly decreased in motor neuronal cultures derived from ALS-patient induced pluripotent stem cells (iPSCs) as well as in the spinal fluids of ALS patients and in the spinal cord of ALS model mice. Impairment of cholesterol synthesis is caused by an increase in toxic function of TDP-43 in ALS.

Introduction

Amyotrophic lateral sclerosis (ALS) is a fatal neurodegenerative disease characterized by selective motor neuronal cell death with cytosolic aggregates(1) mainly consisting of TAR- DNA binding protein of 43 kDa (TDP-43)(2, 3). Clinical studies have shown that dyslipidemia and presymptomatic body fat are associated with the risk and prognosis of ALS patients(4–7). High serum levels of cholesterol, or hyperlipidemia, have been reported to be protective against the prognosis of ALS(8–11), and the presence of hypolipidemia precedes disease progression in ALS model mice(12, 13). In addition, glycolysis upregulation was reported to be protective against ALS progression in a *Drosophila* model of TDP-43 proteinopathy(14). Furthermore, the onset of ALS in patients with antecedent hyperlipidemia is delayed by 6 months(15), and dyslipidemia is presumed to be involved in other neurodegenerative diseases such as Huntington's disease(16).

Past studies that analyzed motor neurons (MNs) derived from induced pluripotent stem cells (iPSCs) generated from familial ALS patients with TDP-43 mutation(17, 18) have reported that TDP-43 was elevated in both RNA and protein levels and that the expression of genes involved in sterol biosynthesis is decreased in ALS MNs with ALS-related mutant TDP-43. Cellular models of TDP-43 proteinopathy exhibited TDP-43 mislocalization in mitochondria and disruption of mitochondrial complex I assembly, suggesting that TDP-43 may play a role in cholesterol metabolisms in ALS(19, 20). In the current study, we analyzed cholesterol metabolisms and associated gene expression profiles regulated by TDP-43 using cellular and mouse models and patient samples.

Methods

Cell culture, plasmids, knockdown

DAP (triple affinity-purification tag; biotin and FLAG tags, and N-terminal epitope tag; 6×histidine) -TDP-43-inducible 293T Rex cells were cultured in Dulbecco's modified Eagle's medium (DMEM, glucose, 4.5 g/liter) supplemented with Tet System Approved FBS (Takara Bio USA, CA, USA) at 37°C in a 5% CO_2/95% air atmosphere. The pSyn-SRE-Luc vector was kindly provided by Dr. Elena Cattaneo (Univ. of Milan), and pFLAG-N-SREBP2 (1-481) was generously given by Dr. Yoshihiro Yoneda (Osaka Univ.). pcDNA3.1-Myc-SREBP2 (1-3423) and pcDNA3.1-TDP-43 (1-1253) were generated using the In-Fusion HD cloning Kit (Takara Bio USA). For the knockdown of TDP-43 and mTOR, we transfected 50 nM and 200 nM mission siRNA (Sigma-Aldrich, St. Louis, MO, USA) into cultured cells using Lipofectamine LTX (Invitrogen, Carlsbad, CA, USA), respectively. The two kinds of siRNA were attempted in order to rule out off-target effects.

Construction of doxycycline-inducible cell lines

To establish a cell line stably expressing DAP-TDP-43 upon doxycycline application, we used an Flp-In T-Rex Expression System (Invitrogen). Flp-In T-Rex 293 cells (293T Rex) were transfected with pOG44 (Invitrogen) and DAP-TDP-43 pcDNA5/FRT/TO and cultured for 48 hours in culture medium containing 200 μg/ml of hygromycin B (Invitrogen)(19).

Gene expression analysis

One hundred ng of total RNA was processed by using the Ambion WT Expression Kit (Life Technologies, Carlsbad, CA, USA) and WT Terminal Labeling and Controls Kit (Affymetrix, Santa Clara, CA, USA) according to the manufacturers' instructions. The sample was then hybridized onto GeneChip Human Transcriptome Array 2.0 (Affymetrix). After washing and staining, the microarray was scanned by GeneChip Scanner 3000 7G (Affymetrix). The sample was re-hybridized onto a GeneChip Human Gene 1.0 ST Array (Affymetrix), and the microarray was washed, stained and scanned. Signal data were analyzed by using Affymetrix Transcriptome Analysis Console software (Affymetrix) for the Human Transcriptome Array and Partek Genomic Suite software (Partek Inc., St. Louis, MO, USA). IPA analysis and gene set analysis for genes found with a fold-change greater than 1.2 were performed using Benjamini Hochberg FDR ($p < 0.05$). The data were analyzed by Genespring GX software (Agilent Technologies, La Jolla, CA, USA) for the gene set analysis.

RNA sequence analysis (RNA-seq)

We extracted total RNA using the RNeasy Plus Kit (QIAGEN, Hilden, Germany). After the depletion of ribosomal RNA by Ribo-Zero Gold (Illumina, San Diego, CA, USA), we prepared libraries using the Illumina TruSeq Stranded Total RNA Sample Prep Kit (Illumina). The libraries were sequenced in the 100 cycle Single-Read mode of HiSeq2500 (Illumina). All sequence reads were extracted in FASTQ format using BCL2FASTQ Conversion Software 1.8.4 in the CASAVA 1.8.4 pipeline. The number of sequence reads is listed in Additional file 1: Table S4. The sequence reads were mapped to hg19 reference genes, downloaded on 10 December 2012, using Tophat v2.0.8b, and quantified by RPKMforGenes, downloaded on 19 October 2012. Gene Ontology analysis was performed by GOstats and GOdb v2.14.0 in R package

3.1.0. To estimate transcript variants, Partek Genomics Suite v6.6 with Gencode v19 reference annotation was used. Mapping was performed using TopHat (CCB at JHU, USA).

Quantitative reverse transcription PCR (qRT-PCR)

QRT-PCR was performed using SYBR green and analyzed with StepOne software v2.1. Primers used for the measurement of SREBP2, TDP-43, HMGCS1, HMGCR, SQLE, LDLR, DHCR24 and LXR mRNA in amplified cDNA from cells are listed in Additional file 1: Table S5. In HEK293T or DAP-TDP-43 293T Rex cells for TDP-43 knockdown, control and TDP-43 siRNA (Sigma-Aldrich) were transfected (50 μM) using RNAiMAX (Invitrogen).

Induced pluripotent stem cells (iPSCs)

Human cDNAs for reprogramming factors were transduced in human dermal fibroblasts with retrovirus (Sox2, Klf4, Oct3/4 and/or c-Myc) or episomal vectors (Sox2, Klf4, Oct3/4, L-Myc, Lin28, shRNA for p53). We used a human control iPSC line (HPS0063) and a familial ALS iPSC line with TDP-43 mutation M337V (A3416). Several days after the transduction, the fibroblasts were harvested and replated on an SNL feeder layer. On the next day, the medium was changed to primate embryonic stem cell medium (Reprocell, Kanagawa, Japan) supplemented with 4 ng/ml bFGF (Wako Chemicals, Osaka, Japan). The medium was changed every other day. Thirty days after the transduction, iPSC colonies were gathered.

Induction of spinal motor neurons by quick embryoid body-like aggregates method (SFEBq)

iPSCs were dissociated to single cells and quickly reaggregated in low cell adhesion U-shaped 96-well plates (Lipidure Coat Plate A-U96, NOF Corporation, Tokyo, Japan). Aggregations were cultured in 5% DFK medium (5% KSR Medium (DFK5%, DMEM/Ham's F12 (Sigma-Aldrich), 5% KSR (Invitrogen), MEM-NEAA (Invitrogen), L-glutamine (Sigma-Aldrich), 2-mercaptoethanol (Wako)) with 2 μM dorsomorphin in a neural inductive stage (P1) for 12 days. After patterning using neurobasal medium supplemented with B27, 1 μM retinoic acid and 100–500 ng/ml Sonic Hedgehog, the aggregates were adhered to Matrigel (BD Biosciences, San Jose, CA, USA)-coated dishes on day 22. Adhesive embryoid bodies were cultured in neurobasal medium with 10 ng/ml BDNF, 10 ng/ml GDNF and 10 ng/ml NT-3 in P2 culture. They were then separated from the dish by Accutase (Sigma-Aldrich), dissociated into a small clump or single cells, and cultured at 500,000 cells/well on Matrigel-coated 24-well dishes on day 35 as the P3 maturation stage.

Immunoblots

Differentiated cells were treated with cytosine arabinoside (AraC) (Sigma-Aldrich). Three days after the removal of AraC, the cells were harvested and lysed in TS buffer (50 mM Tris-HCl buffer, pH 7.5, 0.15 M NaCl, 5 mM ethylenediaminetetraacetic acid, 5 mM ethylene glycol bis (β-aminoethyl ether)-N,N,N,N-tetraacetic acid, and protease inhibitor cocktail (Roche, Basel, Switzerland)] containing 1% Triton X-100 on ice for 10 minutes. After sonication, samples were centrifuged at 10,000 x g for 15 minutes at 4°C. The supernatant was saved as the soluble fraction, and the pellet was resuspended, sonicated in 2% SDS

buffer and saved as the insoluble fraction. Each 10-μg sample of protein was subjected to SDS-PAGE (10–20% polyacrylamide gels, BIO CRAFT, Tokyo, Japan), with or without 2-ME, and separated proteins were transferred to PVDF. The membranes were incubated with primary antibodies, followed by appropriate secondary antibodies, and then visualized using ECL plus or ECL chemiluminescence (GE Healthcare, Chicago, IL, USA). The images were acquired on an LAS 4000 (GE Healthcare). The following primary antibodies were used in this assay: TDP-43 (Protein Tech, 1:1,000), β-actin (Sigma-Aldrich, 1:5,000), SREBP1 (Protein Tech, 1:500), SREBP2 (Cayman Chemical, 1:200), mTOR (Cell Signaling Technology, 1:1000), Raptor (Cell Signaling Technology, 1:1000), Lipin-1 (Cell Signaling Technology, 1:1000), p70S6K (Cell Signaling Technology, 1:1000), and p-p70S6K (Cell Signaling Technology, 1:1000).

Reporter assay

HEK293T cells were transiently transfected with SRE-luciferase reporter construct (pSynSRE, 1.0 μg) and pRL-SV40 (Promega, Madison, WI, USA) (0.2 μg) along with pcDNA3.1-CMV-TDP-43 (0, 0.5, 1.0, 2.0 μg) or pcDNA3.1 (2.0, 1.0, 0.5, 0 μg) using Lipofectamine LTX (Invitrogen). After 72 hours, the cells were lysed for the Luciferase assay. The lysates were measured in triplicate using a Dual Luciferase Reporter Assay System (Promega) on Envision Multilabel Reader (PerkinElmer, Waltham, MA, USA). Relative activity was defined as the ratio of firefly luciferase activity to Renilla luciferase activity to normalize for transfection efficiency.

Mice

We purchased Prp-TDP43A315T mice (B6Cg-Tg (Prnp-TARDBP*A315T) 95Balo/J, 010700) from The Jackson Laboratory (location?). As described previously(21), the asymptomatic stage is between 1–2 months of age. The onset of gait disorder appeared at ∼3 months of age in transgenic mutant TDP-43 mice (symptomatic stage) and increased slightly over the next several months. The animals became paralyzed at ∼5 months of age, corresponding to the end stage (average including males and females); they were unable to move their hindlimbs or right themselves when placed on their backs. For cholesterol measurements, the mice were perfused with cold PBS. All surgical procedures were performed according to the rules set by the Ethics Committee of Kyoto University.

Human spinal fluid samples

For disease diagnosis, we obtained spinal fluid samples by lumbar puncture; initial pressure, cell count, total protein level, and glucose level were measured. The remaining samples were frozen at 80℃ until further investigation. We collected spinal fluids from ALS patients (N = 20) and control patients (N = 20).

Cholesterol measurement

Cells were homogenized in PBS, and the lipids were extracted by modified Bligh and Dyer extraction method for the quantitative analysis of cholesterol(22, 23). Briefly, 100 μl of chloroform plus methanol (2:1) was added to 100 μl of PBS including homogenized cells after counting the cell number. After centrifugation, the chloroform layer was collected and dried with a centrifugal dryer. The dry matter was lysed in 100 μl of ethanol to measure free cholesterol using a Cholesterol Assay kit (Cayman Chemical

Company, Ann Arbor, MI, USA). Fluorescence signals were read with an Envision Multilabel Reader (PerkinElmer). Total lipids including sterols in spinal fluids from patients were extracted by the same method, with the extracts being subjected to LC-MS/MS-based quantification (Agilent 6400). Briefly, 100 µl of chloroform plus methanol (2:1) was added to 10 µl of spinal fluids mixed with 90 µl of PBS. After centrifugation, the chloroform layer was collected and dried with a centrifugal dryer. The dry matter was lysed in 100 µl of ethanol and filtered with a 0.2-µm centrifugal filter tube, and measured for cholesterol by using Agilent 6400.

Statistics

All data are shown as mean ± s.e.m. or ± s.d. The comparison of two groups was analyzed using unpaired two-tailed Student's *t*-test or paired t-test. One-way ANOVA was performed for each comparison followed by Tukey's post hoc tests for the evaluation of pair-wise group differences. A P value < 0.05 was considered statistically significant. Analyses were performed by JMP (SAS Institute Inc., Cary, NC, USA) and Excel Tokei (Social Survey Research Information, Tokyo, Japan).

Results

Gene expression and transcriptome profiling under high levels of TDP-43

A past study using 293T Rex cells stably expressing doxycycline-inductive DAP-TDP-43 reported that mislocalized TDP-43 bound to L-strand transfer RNA of mitochondria and mRNA coding respiratory complex I in mitochondria, disrupting complex I assembly(19). To further investigate the pathogenic role of TDP-43 in 293T Rex cells, we performed gene expression and transcriptome profiling under an overexpressed condition of TDP-43 using expression microarray and RNA deep sequencing. Microarray showed that elevated TDP-43 downregulated the expression of SREBP2 and its downstream genes including HMGCS1, HMGCR and LDLR with significantly decreased cholesterol metabolic process as a gene ontology (GO) term (Fig. 1A and Additional file 1: Table S1). SREBP2 was a top upstream transcriptional regulator of the altered gene expressions caused by TDP-43 (Additional file 1: Table S2). QRT-PCR showed that TDP-43 reduced the mRNA levels of downstream genes of SREBP2 by altering SREBP2 mRNA levels (Fig. 1B). We further performed RNAseq and identified 434 genes that were significantly altered under doxycycline-inductive TDP-43 (Tukey's test, P < 0.05, Additional file 1: Table S3). Among them, elevated TDP-43 significantly decreased the expression levels of HMGCS1, HMGCR, DHCR7 and SREBP2 without biasing the splicing variants of SREBP2 (Fig. 1C-E). Taken together, TDP-43 could regulate SREBP2 by regulating its mRNA expression level.

TDP-43 decreases cholesterol biogenesis by inhibiting SREBP2 activity

Next, we investigated whether TDP-43 could affect the level of SREBP2 protein and its function. We overexpressed or knocked-down TDP-43 in the DAP-TDP-43 293T cell line using small interfering RNA

(siRNA). The overexpression of TDP-43 significantly reduced the mRNA level of SREBP2 (Fig. 2A, B), and western blotting analysis revealed that TDP-43 persistently decreased the amount of the cleaved N-active form of SREBP2 (N-SREBP2) in a TDP-43 expression-dependent manner (Fig. 2C, D). SREBP2 is a critical transcriptional factor that regulates various enzymes in the cholesterol biosynthetic pathway by binding sterol-regulatory elements (SREs) in the promoters of cholesterol-related genes(24, 25). In accordance with the suppressive effect on SREBP2 quantity, TDP-43, through overexpression and knockdown, negatively regulated the endogenous transcriptional activity of SREBP2 as measured with a transfected SRE-luciferase construct (SRE-luc) (Fig. 2E, F). Elevated TDP-43 could inhibit SRE sensitivity to decreased cholesterol level in a fashion similar to authentic sterol-regulated conditions such as cholesterol excess by cholesterol addition or cholesterol depletion by the addition of methyl-beta-cyclodextrin (MbCD) and lovastatin, two HMGCoA reductase inhibitors (Fig. 2G). Subsequently, TDP-43 altered the amount of cholesterol (Fig. 2H).

TDP-43 regulates SREBP2 activity via the mTORC1 signaling pathway

We next analyzed the effect of the regulatory mechanism of TDP-43 on SREBP2 expression. SREBP2 expression is regulated by mTOR Complex 1 (mTORC1) mainly consisting of mTOR, Raptor(26–28), an inhibitor of autophagy, via p70S6 kinase1 (p70S6K), and Lipin-1(29, 30), since a past study demonstrated that TDP-43 could regulate the autophagy-lysosome pathway by mTORC1 activity(31). The mTORC1 pathway is influenced by adenosine triphosphate (ATP) concentration(32). Therefore, we tested the mTORC1 contribution to the TDP-43 regulation of SREBP2 expression as well as the contribution of the activation-status of mTORC1 and its mediators to SREBP2 expression, p70S6K and Lipin-1. We examined the expression level of mTORC1 under doxycycline-induced TDP-43 and found that overexpressed TDP-43 inhibited the expression level of mTOR, Raptor and Lipin-1 48 hours after the TDP-43 induction (Fig. 3A-C). The transcriptional activity of SREBP2 was inhibited by mTOR knockdown or by the mTOR inhibitor rapamycin, but these inhibitory effects were nullified by TDP-43 (Fig. 3D). Finally, an activator of mTORC1, the MEK inhibitor dorsomorphin, rescued the inhibitory effect of TDP-43 on SREBP2 transcriptional activity (Fig. 3E). These results indicated that the inhibitory effect of TDP-43 on SREBP2 is mediated by the mTORC1 signaling pathway.

Decreased cholesterol levels in spinal cord tissue of ALS model mice, ALS-patient iPSC-derived motor neurons and cerebrospinal fluids in ALS patients

Next, we investigated the cholesterol level of spinal cord tissue from ALS model mice overexpressing A315T mutant TDP-43 ($N = 10$)(33). Whole spinal cord tissues from transgenic mice or littermate control mice were fractionated to measure the amount of cholesterol per unit weight. The amounts of both total and free cholesterol were significantly decreased in the spinal cord tissue of transgenic female mice compared to their littermate controls at the pre-symptomatic stage (Fig. 4A), suggesting that TDP-43 could impair cholesterol biosynthesis *in vivo*. To analyze the effect of TDP-43 regulation on cholesterol homeostasis in human motor neurons, we employed ALS motor neuronal cultures derived from patient

iPSC lines with ALS-related TDP-43 mutation M337V(17). As previously reported, the amount of TDP-43 was increased in motor neuronal cultures differentiated from ALS patient iPSCs with TDP-43 mutation compared to control (Fig. 4B). Further, the expression levels of SREBP2 and mTOR were decreased (Fig. 4B), as also were the mRNA levels of SREBP2 and downstream genes (Fig. 4C). The amounts of cholesterol were also decreased in ALS motor neuronal cultures compared to control (Fig. 4D), suggesting that ALS-related mutant TDP-43 decreased cholesterol biogenesis regulated by SREBP2 in human motor neurons. To reveal aberrant cholesterol metabolism in sporadic ALS pathophysiology, we examined the amount of cholesterol in the cerebrospinal fluid (CSF) of sporadic ALS patients (N = 20) and disease-control patients (N = 20) with similar characteristics (Table 1). The cholesterol amounts were significantly decreased in CSF of ALS patients, but not in their serum (Fig. 4E and Tables 2, 3). De novo synthesis is responsible for almost all cholesterol in the central nervous system(34). CSF is in indirect contact with interstitial fluids and reflects biochemical changes in the central nervous system(35), suggesting that the amount of cholesterol in CSF should reflect lipid metabolism in the central nervous system. Collectively, cholesterol metabolism was impaired by TDP-43 in ALS.

Discussion

By translating ALS clinical findings reversely into basic research analysis, we found that TDP-43 protein inhibited the expression of SREBP2 and its transcriptional activity through the mTORC1 signaling pathway, suggesting a potential mechanism for neurodegenerative diseases.

Sterol regulation maintaining cellular cholesterol is critical for cell growth and survival. In general, the SREBP2 pathway is robustly activated during sterol depletion. It has been reported that the level of HMG-CoA reductase is elevated in ALS spinal cord grey matter, that the SREBP2 expression level is declined in ALS model mice with mutant SOD1(36), and that Spinocerebellar Ataxia type 2 model mice harboring TDP-43 pathology exhibit concomitant cholesterol biogenesis suppression(37). Our observations suggest that TDP-43 inhibited the maintenance of the cellular cholesterol level by SREBP2, and that this impaired cholesterol metabolism, which is presumably involved in other neurodegenerative diseases including Alzheimer's disease (AD) and Huntington's disease(16, 38, 39), is crucial in the ALS pathophysiology. A clinical study reported that there was a significant correlation between the CSF level of 24S-hydroxycholesterol and total tau protein in AD patients(40). CYP27A1 associated with cholesterol metabolism has been identified as a susceptible gene for sporadic ALS, and CYP27A1 mutation leading to cerebrotendinous xanthomatosis manifests as an upper motor neuron symptom(41).

We found a modest yet significant difference in total and free cholesterol in the spinal cord between control and ALS model mice, but only in female mice. A previous study revealed that male mice die of bowel obstruction due to gut dysfunction(33), which could have masked the metabolic phenotypes in our study, and with this the cause of death.

We performed a solvent extraction method to measure the amount of free cholesterol in the CSF of ALS patients, finding major metabolites such as 24S-hydroxycholesterol in the brain, which was reported to decrease in the CSF of ALS patients by another study using a solid-phase extraction method(42).

We speculate that a cholesterol complement is not enough to rescue ALS MNs. Olesoxime, which has a cholesterol-like structure, has been thought to be neuroprotective for ALS MNs(43). However, this compound failed in a phase 3 clinical trial for ALS(44), which could underlie the requirement for a concomitant therapy that compensates for cholesterol in ALS MNs. Furthermore, as shown in Huntington's disease, SREBP2 gene therapy may be promising for ALS(45). Taken together, this reverse-translational study provides a molecular basis for the future ALS therapy targeting cholesterol metabolism.

Abbreviations

ALS
Amyotrophic lateral sclerosis
TDP-43
TAR DNA binding protein
RNA-Seq
RNA deep sequencing
SREBP2
Sterol regulatory element-binding protein 2
mTORC1
mTOR Complex I
iPSCs
Induced pluripotent stem cells
MNs
Motor neurons
DAP
Triple affinity-purification tag; biotin and FLAG tags, and N-terminal epitope tag; 6×histidine
siRNA
Small interfering RNA
SREs
Sterol-regulatory elements
SRE-luc
SRE-luciferase construct
MbCD
Methyl-beta-cyclodextrin
p70S6K
p70S6 kinase1
ATP

Adenosine triphosphate
CSF
Cerebrospinal fluid
Dox
Doxycycline
T-Chol
Total cholesterol
FC
Free cholesterol,
TG
Triglyceride
PL
Phospholipid
Tg
Transgenic
non-Tg
non-transgenic
HDL
High density lipoprotein
LDL
Low density lipoprotein
TP
Total protein
A/G
Albumin/globulin ratio
BS
Blood sugar
UA
Uric acid
Fe
Iron.

Declarations

Ethics approval and consent to participate

This study was approved by the Institutional Review Boards of Kyoto University and Tokushima University, and all surgical procedures for animal studies were performed according to the rules set forth by the Ethics Committee of Kyoto University. Written informed consent was received from the participants prior to inclusion in the study. Samples from the participants were identified by numbers, not by names.

Consent for publication

Written informed consent for publication was received from each participant.

Availability of data and materials

All data generated or analyzed during this study are included in this published article and its Additional files.

Competing interests

The authors have declared that no competing interest exists.

Funding

This research was funded in part by a grant for Core Center for iPS Cell Research of Research Center Network for Realization of Regenerative Medicine from AMED to H.I. and the Nakabayashi Trust for ALS Research (N.E.).

Author's contributions

H.I. conceived and planned the project; N.E., H.S., and H.I. designed the experiments; N.E. and H.I. wrote the manuscript; N.E., I.T., K.T., T.E., M.N., A.W., N.M., S.S., T.S., K.K., T.T. and R.T. performed the experiments; Y.I, K.F, and R.K. recruited patients and analyzed their spinal fluids; K.I. and N.T. generated DAP-TDP-43 cell lines.

Acknowledgements

We would like to express our sincere gratitude to all our coworkers and collaborators, and to Dr. Samuel L. Pfaff, Dr. Marta Valenza, Dr. Elena Cattaneo, Dr. Yoshihiro Yoneda for providing plasmids.

References

1. Bruijn LI, Miller TM, Cleveland DW. Unraveling the mechanisms involved in motor neuron degeneration in ALS. Annu Rev Neurosci. 2004;27:723–49.
2. Neumann M, Sampathu DM, Kwong LK, Truax AC, Micsenyi MC, Chou TT, et al. Ubiquitinated TDP-43 in frontotemporal lobar degeneration and amyotrophic lateral sclerosis. Science. 2006;314(5796):130–3.
3. Arai T, Hasegawa M, Akiyama H, Ikeda K, Nonaka T, Mori H, et al. TDP-43 is a component of ubiquitin-positive tau-negative inclusions in frontotemporal lobar degeneration and amyotrophic lateral sclerosis. Biochem Biophys Res Commun. 2006;351(3):602–11.
4. Gallo V, Wark PA, Jenab M, Pearce N, Brayne C, Vermeulen R, et al. Prediagnostic body fat and risk of death from amyotrophic lateral sclerosis: the EPIC cohort. Neurology. 2013;80(9):829–38.

5. Huisman MH, Seelen M, van Doormaal PT, de Jong SW, de Vries JH, van der Kooi AJ, et al. Effect of Presymptomatic Body Mass Index and Consumption of Fat and Alcohol on Amyotrophic Lateral Sclerosis. JAMA Neurol. 2015;72(10):1155–62.
6. Jawaid A, Khan R, Polymenidou M, Schulz PE. Disease-modifying effects of metabolic perturbations in ALS/FTLD. Mol Neurodegener. 2018;13(1):63.
7. Mariosa D, Hammar N, Malmstrom H, Ingre C, Jungner I, Ye W, et al. Blood biomarkers of carbohydrate, lipid, and apolipoprotein metabolisms and risk of amyotrophic lateral sclerosis: A more than 20-year follow-up of the Swedish AMORIS cohort. Ann Neurol. 2017;81(5):718–28.
8. Dorst J, Kuhnlein P, Hendrich C, Kassubek J, Sperfeld AD, Ludolph AC. Patients with elevated triglyceride and cholesterol serum levels have a prolonged survival in amyotrophic lateral sclerosis. J Neurol.258(4):613–7.
9. Dupuis L, Corcia P, Fergani A, Gonzalez De Aguilar JL, Bonnefont-Rousselot D, Bittar R, et al. Dyslipidemia is a protective factor in amyotrophic lateral sclerosis. Neurology. 2008;70(13):1004–9.
10. Chio A, Calvo A, Ilardi A, Cavallo E, Moglia C, Mutani R, et al. Lower serum lipid levels are related to respiratory impairment in patients with ALS. Neurology. 2009;73(20):1681–5.
11. Zhang L, Tang L, Huang T, Fan D. Life Course Adiposity and Amyotrophic Lateral Sclerosis: A Mendelian Randomization Study. Ann Neurol. 2020;87(3):434–41.
12. Fergani A, Oudart H, Gonzalez De Aguilar JL, Fricker B, Rene F, Hocquette JF, et al. Increased peripheral lipid clearance in an animal model of amyotrophic lateral sclerosis. Journal of lipid research. 2007;48(7):1571–80.
13. Kim SM, Kim H, Kim JE, Park KS, Sung JJ, Kim SH, et al. Amyotrophic lateral sclerosis is associated with hypolipidemia at the presymptomatic stage in mice. PLoS One. 2011;6(3):e17985.
14. Manzo E, Lorenzini I, Barrameda D, O'Conner AG, Barrows JM, Starr A, et al. Glycolysis upregulation is neuroprotective as a compensatory mechanism in ALS. Elife. 2019;8.
15. Hollinger SK, Okosun IS, Mitchell CS. Antecedent Disease and Amyotrophic Lateral Sclerosis: What Is Protecting Whom? Front Neurol. 2016;7:47.
16. Valenza M, Rigamonti D, Goffredo D, Zuccato C, Fenu S, Jamot L, et al. Dysfunction of the cholesterol biosynthetic pathway in Huntington's disease. The Journal of neuroscience: the official journal of the Society for Neuroscience. 2005;25(43):9932–9.
17. Egawa N, Kitaoka S, Tsukita K, Naitoh M, Takahashi K, Yamamoto T, et al. Drug screening for ALS using patient-specific induced pluripotent stem cells. Science translational medicine. 2012;4(145):145ra04.
18. Inoue H, Yamanaka S. The use of induced pluripotent stem cells in drug development. Clin Pharmacol Ther. 2011;89(5):655–61.
19. Izumikawa K, Nobe Y, Yoshikawa H, Ishikawa H, Miura Y, Nakayama H, et al. TDP-43 stabilises the processing intermediates of mitochondrial transcripts. Sci Rep. 2017;7(1):7709.

20. Wang W, Wang L, Lu J, Siedlak SL, Fujioka H, Liang J, et al. The inhibition of TDP-43 mitochondrial localization blocks its neuronal toxicity. Nat Med. 2016;22(8):869–78.
21. Wegorzewska I, Bell S, Cairns NJ, Miller TM, Baloh RH. TDP-43 mutant transgenic mice develop features of ALS and frontotemporal lobar degeneration. Proc Natl Acad Sci USA. 2009;106(44):18809–14.
22. Folch J, Lees M, Sloane Stanley GH. A simple method for the isolation and purification of total lipides from animal tissues. J Biol Chem. 1957;226(1):497–509.
23. Matsuzawa N, Takamura T, Kurita S, Misu H, Ota T, Ando H, et al. Lipid-induced oxidative stress causes steatohepatitis in mice fed an atherogenic diet. Hepatology. 2007;46(5):1392–403.
24. Brown MS, Goldstein JL. The SREBP pathway: regulation of cholesterol metabolism by proteolysis of a membrane-bound transcription factor. Cell. 1997;89(3):331–40.
25. Shimano H, Sato R. SREBP-regulated lipid metabolism: convergent physiology - divergent pathophysiology. Nat Rev Endocrinol. 2017;13(12):710–30.
26. Wang BT, Ducker GS, Barczak AJ, Barbeau R, Erle DJ, Shokat KM. The mammalian target of rapamycin regulates cholesterol biosynthetic gene expression and exhibits a rapamycin-resistant transcriptional profile. Proc Natl Acad Sci USA. 2011;108(37):15201–6.
27. Xiao X, Song BL. SREBP: a novel therapeutic target. Acta Biochim Biophys Sin. 2013;45(1):2–10.
28. Ma KL, Liu J, Wang CX, Ni J, Zhang Y, Wu Y, et al. Activation of mTOR modulates SREBP-2 to induce foam cell formation through increased retinoblastoma protein phosphorylation. Cardiovascular research. 2013;100(3):450–60.
29. Peterson TR, Sengupta SS, Harris TE, Carmack AE, Kang SA, Balderas E, et al. mTOR complex 1 regulates lipin 1 localization to control the SREBP pathway. Cell. 2011;146(3):408–20.
30. Duvel K, Yecies JL, Menon S, Raman P, Lipovsky AI, Souza AL, et al. Activation of a metabolic gene regulatory network downstream of mTOR complex 1. Molecular cell. 2010;39(2):171–83.
31. Xia Q, Wang H, Hao Z, Fu C, Hu Q, Gao F, et al. TDP-43 loss of function increases TFEB activity and blocks autophagosome-lysosome fusion. EMBO J. 2016;35(2):121–42.
32. Dennis PB, Jaeschke A, Saitoh M, Fowler B, Kozma SC, Thomas G. Mammalian TOR: a homeostatic ATP sensor. Science. 2001;294(5544):1102–5.
33. Hatzipetros T, Bogdanik LP, Tassinari VR, Kidd JD, Moreno AJ, Davis C, et al. C57BL/6J congenic Prp-TDP43A315T mice develop progressive neurodegeneration in the myenteric plexus of the colon without exhibiting key features of ALS. Brain Res. 2014;1584:59–72.
34. Dietschy JM, Turley SD. Thematic review series: brain Lipids. Cholesterol metabolism in the central nervous system during early development and in the mature animal. Journal of lipid research. 2004;45(8):1375–97.
35. Segal MB. The choroid plexuses and the barriers between the blood and the cerebrospinal fluid. Cell Mol Neurobiol. 2000;20(2):183–96.

36. Dodge JC, Jensen EH, Yu J, Sardi SP, Bialas AR, Taksir TV, et al. Neutral Lipid Cacostasis Contributes to Disease Pathogenesis in Amyotrophic Lateral Sclerosis. The Journal of neuroscience: the official journal of the Society for Neuroscience. 2020;40(47):9137–47.
37. Canet-Pons J, Sen NE, Arsovic A, Almaguer-Mederos LE, Halbach MV, Key J, et al. Atxn2-CAG100-KnockIn mouse spinal cord shows progressive TDP43 pathology associated with cholesterol biosynthesis suppression. Neurobiol Dis. 2021;152:105289.
38. Mohamed A, Saavedra L, Di Pardo A, Sipione S, Posse de Chaves E. beta-amyloid inhibits protein prenylation and induces cholesterol sequestration by impairing SREBP-2 cleavage. The Journal of neuroscience: the official journal of the Society for Neuroscience. 2012;32(19):6490–500.
39. Karasinska JM, Hayden MR. Cholesterol metabolism in Huntington disease. Nature reviews Neurology. 2011;7(10):561–72.
40. Leoni V, Solomon A, Lovgren-Sandblom A, Minthon L, Blennow K, Hansson O, et al. Diagnostic power of 24S-hydroxycholesterol in cerebrospinal fluid: candidate marker of brain health. Journal of Alzheimer's disease: JAD. 2013;36(4):739–47.
41. Diekstra FP, Saris CG, van Rheenen W, Franke L, Jansen RC, van Es MA, et al. Mapping of gene expression reveals CYP27A1 as a susceptibility gene for sporadic ALS. PLoS One. 2012;7(4):e35333.
42. Abdel-Khalik J, Yutuc E, Crick PJ, Gustafsson JA, Warner M, Roman G, et al. Defective cholesterol metabolism in amyotrophic lateral sclerosis. Journal of lipid research. 2017;58(1):267–78.
43. Martin LJ. Olesoxime, a cholesterol-like neuroprotectant for the potential treatment of amyotrophic lateral sclerosis. IDrugs: the investigational drugs journal. 2010;13(8):568–80.
44. Lenglet T, Lacomblez L, Abitbol JL, Ludolph A, Mora JS, Robberecht W, et al. A phase II-III trial of olesoxime in subjects with amyotrophic lateral sclerosis. Eur J Neurol. 2014;21(3):529–36.
45. Birolini G, Verlengia G, Talpo F, Maniezzi C, Zentilin L, Giacca M, et al. SREBP2 gene therapy targeting striatal astrocytes ameliorates Huntington's disease phenotypes. Brain: a journal of neurology. 2021.

Tables

Table 1: Characteristics of study participants

Characteristics		ALS patients (*N* = 20)	Control (*N* = 20)	*P* value
		n (%)		
Sex	male	12 (60)	14 (70)	0.774
Age (years)	mean (S.D.)	62.2 (12.4)	61.9 (14.1)	0.570
	median (range)	64.0 (32-81)	59.0 (27-84)	
Diabetes	present	5 (25)	6 (30)	0.802
	borderline	1 (5)	0	
	unknown	14	14	
Treatment of hyperlipidemia	received	4 (20)	4 (20)	1.000

Table 2: Cerebrospinal fluid data between ALS patients and controls

		ALS patients (*N* = 20)	Control (*N* = 20)	*P* value
Cholesterol	mean (S.D.)	2.33 (2.35)	3.96 (4.11)	0.0193*
	median (range)	1.98 (0.17-10.5)	2.77 (0.50-18.9)	
Protein	mean (S.D.)	36.0 (10.3)	66.0 (3.05)	< 0.0001*
	median (range)	34.0 (19-59)	42.5 (26-303)	
Glucose	mean (S.D.)	76.3 (22.7)	77.7 (25.8)	0.586
	median (range)	67.5 (53-150)	69.5 (52-164)	
Cell	mean (S.D.)	3.45 (3.72)	5.16 (4.89)	0.246
	median (range)	2.5 (0-17)	3.0 (0-17)	

Table 3: Serological data between ALS patients and controls

		ALS patients (*N* = 20)	Control (*N* = 20)	*P* value
Cholesterol	mean (S.D.)	198 (26.4)	189 (34.7)	0.251
	median (range)	195 (142-236)	179 (136-264)	
Triglyceride	mean (S.D.)	149 (69.1)	125 (81.7)	0.477
	median (range)	128.5 (60-291)	104.5(48-321)	
HDL	mean (S.D.)	51.2 (19.6)	46.1(14.4)	0.228
	median (range)	48.5 (28-107)	42.0 (28-80)	
LDL	mean (S.D.)	114 (29.3)	95.4 (37.2)	0.110
	median (range)	112 (70-167)	91.5 (35-154)	
TP	mean (S.D.)	7.00 (0.66)	7.23 (0.91)	0.169
	median (range)	6.95 (6.2-8.8)	7.30 (4.9-8.8)	
Albumin	mean (S.D.)	3.86 (0.34)	3.75 (0.54)	0.046*
	median (range)	3.90 (3.3-4.5)	3.70 (1.9-4.4)	
A/G	mean (S.D.)	1.33 (0.38)	1.16 (0.26)	0.111
	median (range)	1.35 (0.60-1.99)	1.20 (0.63-1.58)	
BUN	mean (S.D.)	14.5 (3.90)	15.8 (5.89)	0.083
	median (range)	14.0 (10-28)	15.0 (6-27)	
Creatinine	mean (S.D.)	0.59 (0.16)	0.88 (0.62)	< 0.0001*
	median (range)	0.55 (0.28-0.92)	0.65 (0.39-2.88)	
BS	mean (S.D.)	123 (44.1)	143 (82.0)	0.010*
	median (range)	106 (87-239)	119(82-420)	
UA	mean (S.D.)	5.28 (1.44)	6.69 (6.70)	< 0.0001*
	median (range)	5.3 (2.9-8.6)	5.2 (2.0-30.0)	
IgG	mean (S.D.)	1223 (521)	1351 (339)	0.104
	median (range)	1165 (707-2961)	1223 (972-2171)	
Fe	mean (S.D.)	98.5 (50.1)	92.8 (49.6)	0.987
	median (range)	98 (16-203)	94 (28-212)	
Ferritin	mean (S.D.)	209 (162)	209 (182)	0.673
	median (range)	169 (12-720)	162 (15-746)	

Abbreviations: HDL: high density lipoprotein; LDL: low density lipoprotein; TP: total protein; A/G: albumin/globulin ratio; BS: blood sugar; UA: uric acid; Fe: iron.

Figures

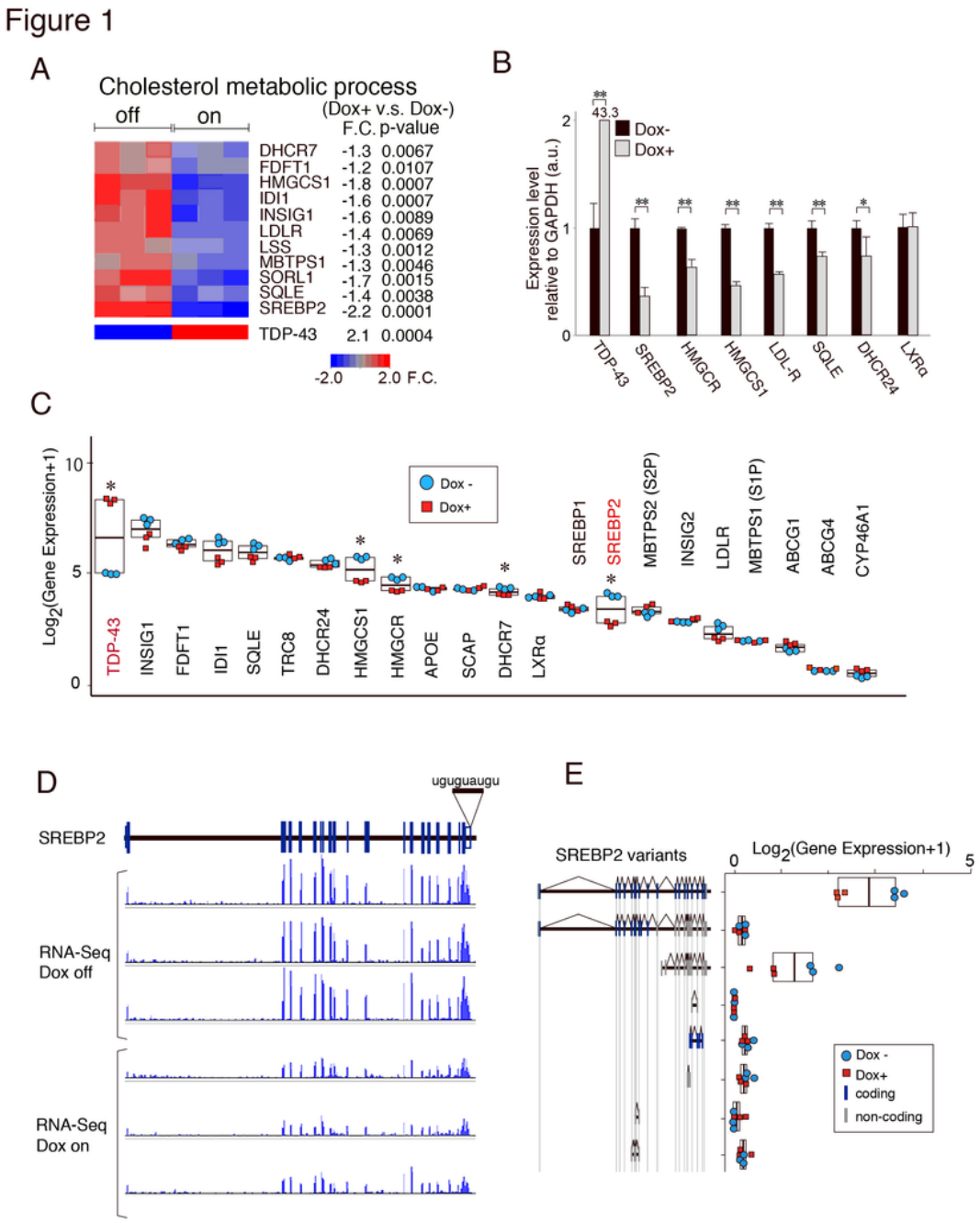

Figure 1

Gene expression and transcriptome profiling under TDP-43 induction. A, A heat map showing decreased genes related to the cholesterol metabolic process under TDP-43-overexpressed condition in the expression microarray in HEK293T Rex cells stably expressing doxycycline (Dox)-induced DAP-TDP-43 (Dox on (+, N = 3) vs. off (-, N = 3) condition, fold change (F.C.) < -1.2). B, QRT-PCR showed that mRNA levels of target genes of SREBP2 were decreased under TDP-43-overexpressed condition. *P < 0.05, **P < 0.01, t-test, error bars = s.d. For each independent experiment, N = 3. C, Deep RNA sequencing analysis (each N = 3) of genes related to cholesterol metabolism. Tukey, *P value < 0.05. D, RNA-seq reads under Dox on or off condition. E, Transcript variants of SREBP2 under Dox on or off condition.

Figure 2

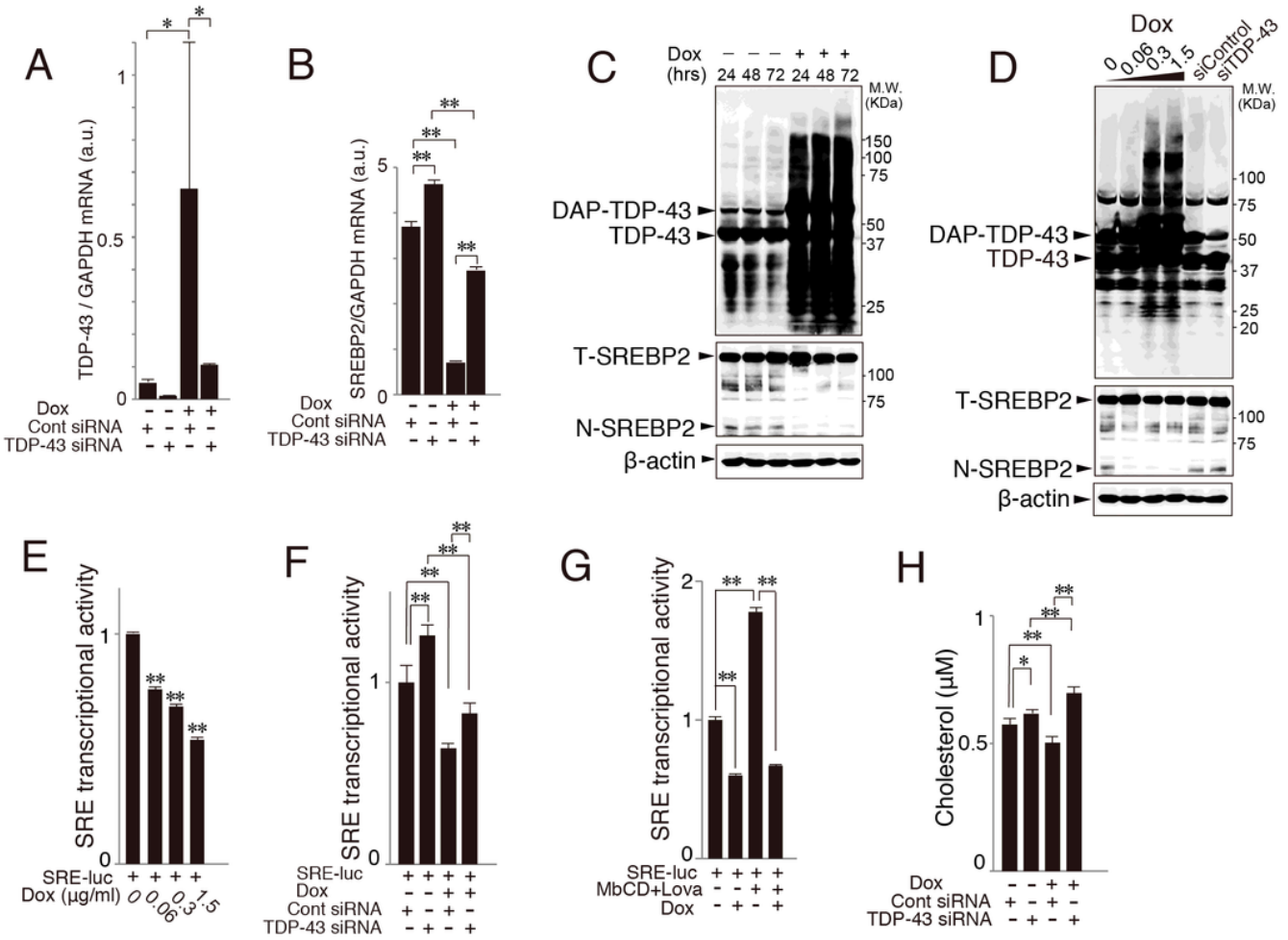

Figure 2

TDP-43 inhibits SREBP2 transcriptional activity via sterol-regulatory elements. A-B, HEK293T Rex cells stably expressing doxycycline (Dox)-induced DAP-TDP-43 treated with Dox or TDP-43 siRNA transfection were lysed and subjected to QRT-PCR (each N = 3) to detect the mRNA levels of TDP-43 (A) and SREBP2 (B) relative to GAPDH. C-D, Immunoblots of lysates from 293T Rex cells treated with Dox or TDP-43 siRNA transfection (N = 3). The expression level of N-SREBP2 at the indicated times (C) was dependent

on the TDP-43 expression level 48 hours after Dox (1.5 μM) treatment (D). E-G, 293T Rex cells were transfected with pSyn-SRE-Luc and pRL-SV40 and lysed for the dual-luciferase assay to detect sterol-regulatory element (SRE)-activity. **P < 0.01, one-way ANOVA (E), two-way ANOVA (F, G). H, Amounts of free cholesterol in 293T Rex cells (1×106) 48 hours after transfection with or without TDP-43 siRNA. *P < 0.05, **P < 0.01, two-way ANOVA, error bars = s.d. For each assay performed, N = 3.

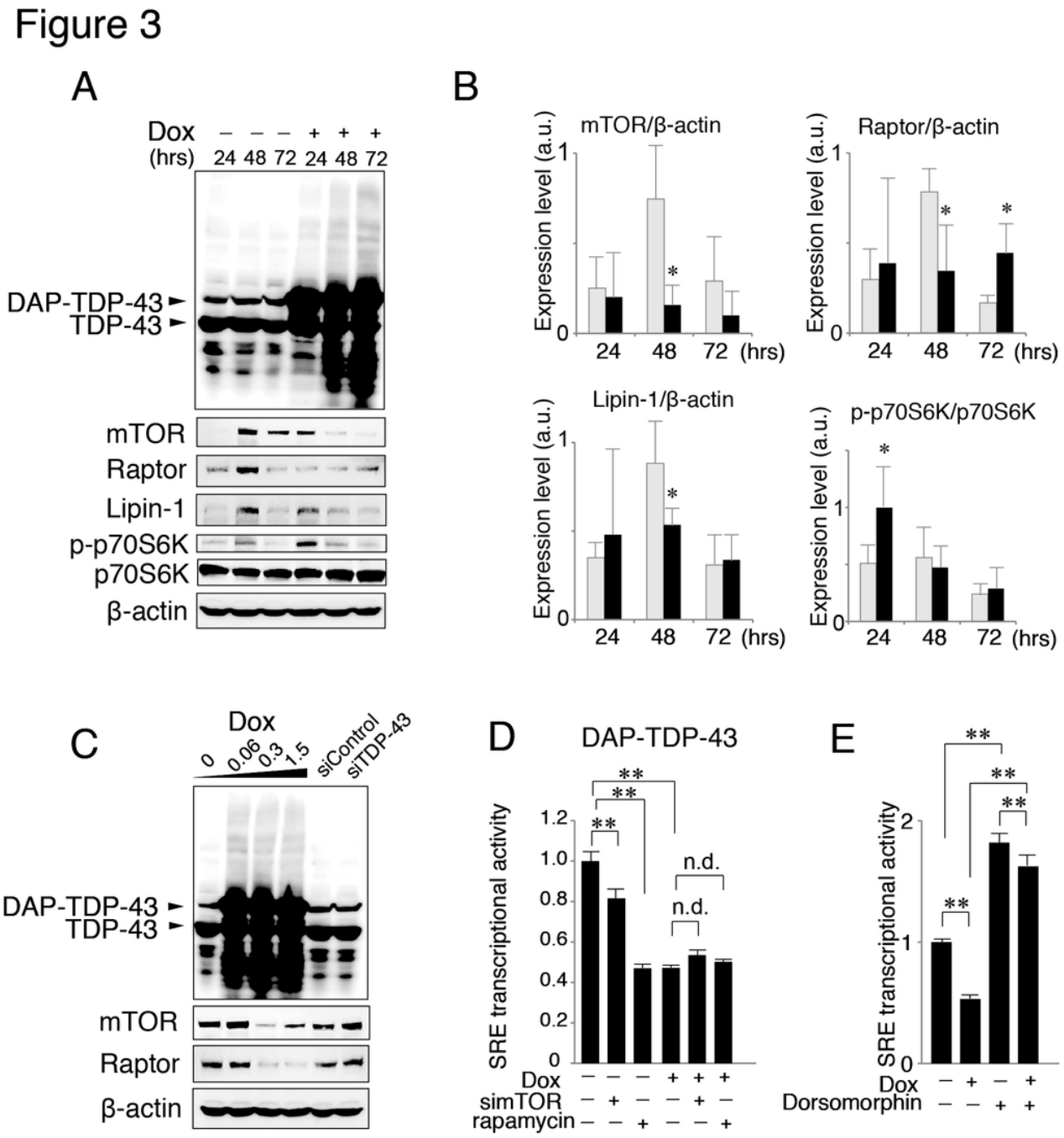

Figure 3

TDP-43 inhibits SREBP2 by mTORC1 signaling. A-C, Immunoblots of lysates from 293T Rex cells treated with doxycycline (Dox, 1.5 μM) or TDP-43 siRNA transfection. The expression level of mTOR, Raptor and

Lipin-1 at the indicated times (A, B) was dependent on the TDP-43 expression level 48 hours after Dox treatment (C). *P < 0.05, t-test, error bars = s.d. Independent blot experiments were performed for quantification (N = 3). D-E, DAP-TDP-43 293T Rex cells were transfected with pSyn-SRE-Luc and pRL-SV40 and lysed for the dual-luciferase assay to detect sterol-regulatory element (SRE)-activity 48 hours after transfection with mTOR siRNA, Dox (1.5 μM), rapamycin (100 nM), or dorsomorphin (100 μM) treatment. **P < 0.01, one-way ANOVA, error bars = s.d. n.d. = 'non-significant difference'. For each assay, N =3.

Figure 4

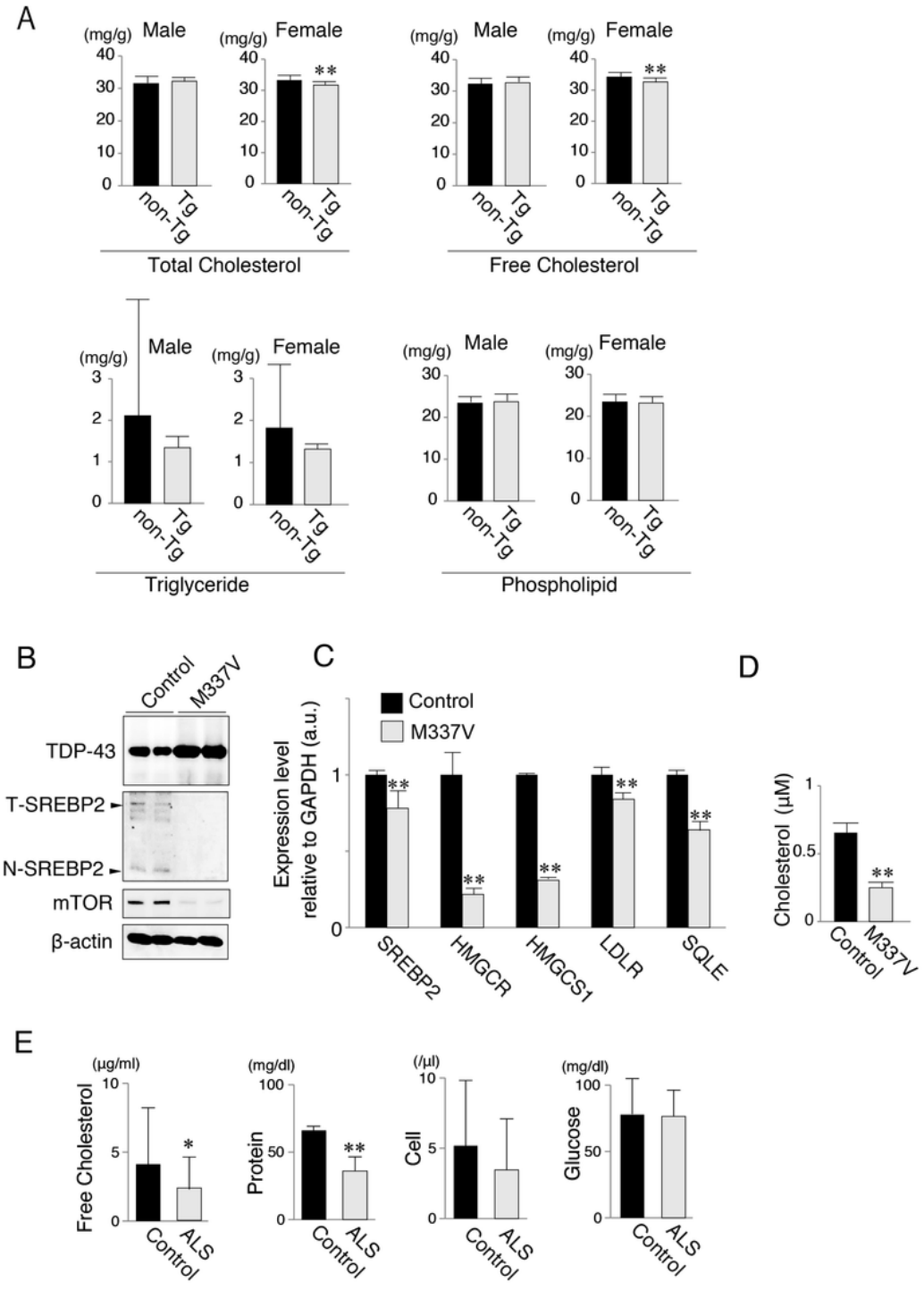

Figure 4

Decreased cholesterol level in spinal cord tissue of ALS model mouse, ALS-patient iPSC-derived motor neurons and spinal fluids of ALS patients. A, The amounts of total cholesterol (T-Chol), free cholesterol (FC), triglyceride (TG) and phospholipid (PL) per g of total spinal cord tissue were measured at 24 weeks after birth in A315T TDP-43 transgenic (Tg) / non-transgenic (non-Tg) male / female mice (N = 10, each group). **P < 0.01, t-test, error bars = s.d. B, Immunoblots (N = 3) of lysates from motor neuronal cultures derived from control and ALS (M337V TDP-43 mutation) iPSCs. C, QRT-PCR (N = 4) for mRNA levels of SREBP2 and its target genes. **P < 0.01, t-test, error bars = s.d. D, The amounts of free cholesterol in motor neuronal cultures (1×106) day 50 after differentiation. **P < 0.01, t-test, error bars = s.d. N = 3. E, Cholesterol levels in spinal fluids of control (N = 20) and ALS patients (N = 20). *P < 0.05, **P < 0.01, t-test, error bars = s.d.

Supplementary Files

This is a list of supplementary files associated with this preprint. Click to download.

- Additionalfile1.docx